IEEE Access
Multidisciplinary ⋮ Rapid Review ⋮ Open Access Journal

Received February 8, 2022, accepted February 23, 2022, date of publication March 16, 2022, date of current version March 23, 2022.

Digital Object Identifier 10.1109/ACCESS.2022.3159243

Programmable High Integration and Resolution Digital Microfluidic Device Driven by Thin Film Transistor Arrays

ZHIJIE LUO[1,2], JIAZHI XU[1], ZHONGYU PAN[1], HANG YIN[1,2], LIANG CAO[1], GUOFU ZHOU[3], AND SHUANGYIN LIU[1,2]

[1]College of Information Science and Technology, Zhongkai University of Agriculture and Engineering, Guangzhou 510225, China
[2]Intelligent Agriculture Engineering Research Center, Guangdong Higher Education Institutes, Zhongkai University of Agriculture and Engineering, Guangzhou 510225, China
[3]Institute of Electronic Paper Displays, South China Academy of Advanced Optoelectronics, South China Normal University, Guangzhou 510006, China

Corresponding author: Hang Yin (yinhangzkj@163.com)

This work was supported in part by the National Natural Science Foundation of China under Grant 61871475, in part by the Guangdong Science and Technology Plan under Grant 201905010006, in part by the Foundation for High-level Talents in Higher Education of Guangdong Province under Grant 2017GCZX001 and Grant 2017KQNCX097, in part by the Guangzhou Science Research Plan under Grant 201904010233 and Grant 201903010043, and in part by the Guangdong Natural Science Foundation under Grant 2021A1515011605.

ABSTRACT A digital microfluidic (DMF) system based on electrowetting on dielectrics (EWOD) is a new technology that is able to manipulate microlitre droplets on the plane. Conventional EWOD devices have difficulty achieving high integration and a large number of electrodes due to the limitation of electrical connections. To realize the precise control of multiple droplets in a large-area EWOD device, we propose a programmable high integration and resolution DMF device based on a thin film transistor array (TFTA) – EWOD in this paper. The TFTA backplane with thousands of individually addressable electrodes used in electrowetting displays (EWDs) is integrated into this device. A source integrated circuit (IC) and a gate IC are bonded on the substrate glass of the device as the driver chip. A TFTA-EWOD device with 320×240 electrodes is designed, fabricated and tested in our experiments. Furthermore, a matching droplet control system with detection and feedback functions was developed and implemented. This system is capable of detecting and analysing individual droplet status while concurrently continuing with other droplet manipulations on the TFTA-EWOD device. The experimental results show that different droplet manipulations, including dispensing, merging and transport, can be carried out successfully on this device. We also successfully applied the proposed device and system to a colorimetric enzymatic assay to show that the proposed scheme is capable of chemical analysis experiments. There are no additional errors introduced by the proposed TFTA-EWOD device. The designed device and matching system proposes a programmable high integration, high resolution, and universal solution for complex DMF applications. We hope that the proposed device and system can provide an experimental platform to other research teams who focus on DMF applications.

INDEX TERMS Electrowetting on dielectric, digital microfluidic, thin film transistor array, integration.

I. INTRODUCTION

Digital microfluidics (DMF) enables the manipulation of droplets on an electrode array surface by applying sufficient voltage. DMF chas several advantages of avoiding cross contamination between different liquids, greatly reducing human interference and chemical reaction time. Additionally, most DMF devices have a simple system structure [1]–[3]. It saves the trouble of making micro-pumps and easily realizes integration.

The DMF system can manipulate and control individual droplets on a planar array of electrodes by applying various control mechanisms, such as electrostatic [4], acoustic wave [5], temperature gradient [6], and electrowetting on dielectric (EWOD) [7]. Among them, the most promising technology for droplet microfluidics

The associate editor coordinating the review of this manuscript and approving it for publication was Karol Malecha.

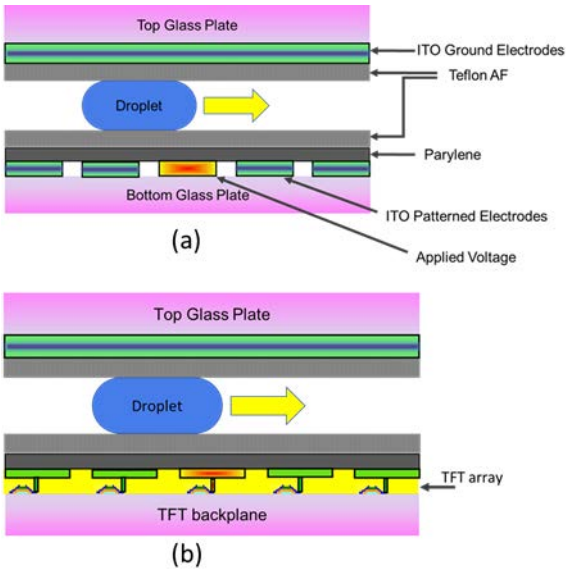

FIGURE 1. (a) EWOD based droplet driving principle. (b) Schematic diagram of the proposed TFTA-EWOD device.

that has emerged within the last decade may be the EWOD [8], [9].

With the EWOD control mechanism, droplets are driven to move on a two dimensional electrode array by using sufficient driving voltage to the individual electrodes. When an electrode of EWOD device is energized, the droplet is pulled to the energized electrode by the EWOD forces (shown in Figure 1(a)). For conventional EWOD devices, the bottom substrate consists of a patterned conductive layer forming an array of individual electrodes [10]. To reduce friction, some EWOD device used silicone oil as the lubricant in previous studies [11]. In recent years, there has been much progress in the research of EWOD devices [12], [13]. Many droplet manipulations [14] and applications have been demonstrated in this type of EWOD device, such as DNA detection [15], enzymatic and immunoassays [16], biomedical applications [17], and cell-based screening [18].

Common and mainstream EWOD chips can achieve electronically reconfigurable 2-D motions on device surfaces [19]–[21]. For this type of EWOD device, 2-D addressable driving units arrays are capable of addressing control each unit independently in an $X_{\mathrm{Rows}} \times Y_{Columns}$ driving electrode array (X_{Rows} is the number of row electrodes, $Y_{Columns}$ is the number of column electrodes) for most droplet applications (e.g., droplet movement and splitting) [22]. This means that the EWOD device needs $X_{\mathrm{Rows}} \times Y_{Columns}$ electrical wires that connect the electrode array to the external driving circuit. Such device design has some application limitations. These electrode array structure of EWOD devices are usually simple, for example, a linear pathway of driving electrodes enabling droplet motion along a single linear path or multiple electrodes driven simultaneously from the same voltage trigger unit. This means that complex droplet splitting and merging operations (e.g., a number of droplets are moving on an EWOD device) are difficult to achieve on the traditional EWOD devices.

Joo Hyon Noh demonstrated the use of thin film transistor arrays as an active matrix addressing method to control an electrofluidic array [23]. However, this device is connected to a separate, conventional ten electrode EWOD array. This work still does not provide a high integration and large format EWOD device on a transparent TFT platform. Furthermore, Hadwen proposed a large format active matrix-EWOD device for combined droplet manipulation and capacitive sensing [24]. However, this device did not integrate gate and source drivers. It uses an expanded designed printed circuit board (PCB) to generate the drive voltages and timing signals supplied to the TFT backplane. Recently, Shaik et al investigated the possibility of using TFT array devices for high-throughput cell manipulation using EWOD [25]. In this paper, it has been demonstrated that the DMF system based on EWOD technique could be used to transport, dispense and merge droplets on TFTA-EWOD devices without damaging the tissue structure contained within. Impedance measurement is used as a droplet tracking mechanism in this control system. This tracking mechanism is mature and widely used for droplet location of traditional EWOD devices. However, an EWOD device based on a TFT array has the characteristics of a small size and a large number of electrodes (which are advantages). Therefore, the efficiency and accuracy of this droplet tracking mechanism are greatly reduced.

In this paper, we describe a programmable high integration and resolution TFTA-EWOD. The proposed device has 76800 (320 × 240) independent addressable drive units. The size of each unit is 150μm × 150μm. Such a design has a higher resolution and larger format than the previous EWOD devices. A high density and larger format matrix driven by TFTA also expands the area and mode of fluid movement, permitting the shape of droplets to be varied and reducing the probability of droplets sticking in a certain path.

The proposed device has high integration. A source integrated circuit (IC) and gate IC are integrated on the substrate glass of this device as a driver chip. The device can be driven as long as the voltage and corresponding timing are provided. Users can control the movement of multiple droplets on this device based on a PC or embedded platform.

Furthermore, a matching droplet control system with detection and feedback functions is developed and implemented. In previous studies, most droplet control system used the equivalent capacitance model to detect the droplet position [26], [27]. This droplet detection scheme is easy to implement but inefficient. Especially for complex EWOD devices, much system memory and running time is required to store many capacitance values for analysis. In contrast with the previous control system, the driver module of proposed control system adopts an embedded architecture. Machine vision measurement is used as the droplet detection mechanism. Such a design has higher portability, efficiency and accuracy. This system is capable of detecting and

analysing individual droplet position, volume, velocity and motion failures while concurrently continuing with other fluid manipulations on a TFTA-EWOD device. The proposed control system can provide a mature and reliable experimental platform or scheme for other EWOD researchers. Several important droplet applications are successfully carried out and demonstrated in the proposed TFTA-EWOD device and matching system.

To show the practicability and generality of our scheme, we successfully applied it to control an enzymatic assay that uses the machine vision-based detection system to analyse the enzymatic product without adding any other external sensors. Compared with a conventional EWOD device, no additional bugs were introduced by the proposed TFTA-EWOD device.

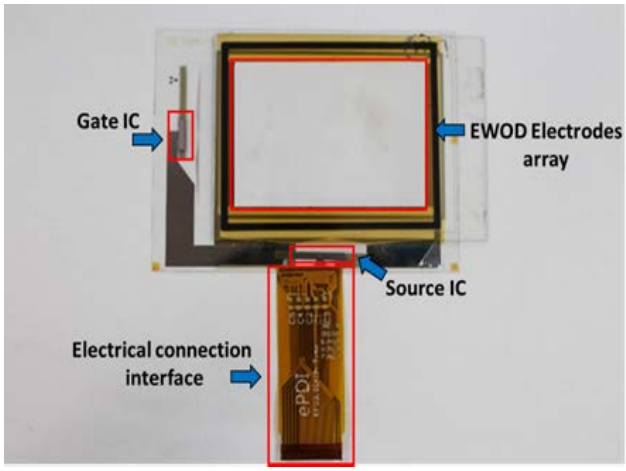

FIGURE 2. Photograph of the entire TFTA-EWOD device.

II. METHODS AND EXPERIMENTS

A. TFTA-EWOD DEVICE DESIGN

A schematic diagram of the proposed TFTA-EWOD device is shown in Figure 1(b). A TFTA backplane with thousands of individually addressable electrodes applied to electrowetting displays (EWDs) is used in the proposed device. The driving characteristics (high voltage driven) and structure (electrowetting) of an EWD device are similar to those of the EWOD device. Therefore, it is extremely well suited for the TFTA-EWOD device.

The TFTA-EWOD device comprises a lower plate (an electrode array) with an upper plane connected parallel to it. The dielectric insulator and hydrophobic layers are processed on top of the TFT array substrate and top glass plate. In proposed scheme, Teflon AF 1600 (800 nm) is used as the hydrophobic and dielectric layer in the proposed TFTA-EWOD device. Through previous experiments we can know that Teflon AF 1600 is a biocompatible polymer with an average static contact angle of 116°. The dielectric constant of Teflon AF 1600 may reached 2.6. Both of these characteristics are very suitable for various droplet manipulations (e.g., dispense, transport) [28]. The lower plate of this device consists of 76800 independent addressable drive electrodes (or units). The size of each drive unit is 150 μm $\times$150 μm, and the separation between drive units is 18 μm. The bottom plate and the upper plate of TFTA-EWOD device are assembled by using a double tape of known thickness as a spacer. Multiple individual droplets are injected into the space contained by the upper and lower plates. If there are dust or particles on the surface of the device, droplet driving for a long time damages the Teflon AF. The process of device preparation should be carried out in a clean room as much as possible.

A photograph of the entire TFTA-EWOD device containing the gate, source IC and electrical connection interface is shown in Figure 2. A gate and source IC that are designed with a programmable display waveform for fitting with the EWD technology are integrated on the substrate glass of this device as a driver chip.

B. PORTABLE ELECTRONIC CONTROL SYSTEM

A high-performance EWOD electronic control system should be portable and highly integrated. A schematic diagram of the proposed portable electronic control system is shown in Figure 3. It is composed of a control module and driving module. The main function of the control module (Cortex-A9) is to process the image of the EWOD device and analyse the droplet positions. Compared with conventional EWOD devices, there are many drive units in the TFTA-EWOD devices, which makes it difficult to locate the droplet positions by the capacitance-based method (as the position time is long and a large number of sensors are needed). The system, with a camera, provides a low-cost and accurate machine vision-based droplet detection scheme. To implement this scheme, a Linux system is embedded into the hardware to realize multithreading. Moreover, a user control interface based on OPENCV and QT is developed on this platform. An FPGA (Cyclone V) is used as the driving core of the proposed system to generate the appropriate control and timing signals for the TFTA-EWOD device. The LCD interface is used as the communication interface between the control module and driving module. The drive mode of the droplets on the TFTA-EWOD device is ''image-driven'', considering the characteristics of the TFTA-EWOD device. The TFTA-EWOD device can be seen as a display screen. The drive unit of the device is a ''display pixel''. Every drive time of the TFTA-EWOD device corresponds to a new image refresh.

The portable electronic control system is designed to manage a range of EWOD device electrode actuations and obtain droplet positions from the droplet detection system to realize the actuation sequence and logic for the next drive phase.

C. DROPLETS DETECTION SYSTEM

To accurately control the droplets, we proposed droplet detection software based on machine vision for the TFTA-EWOD

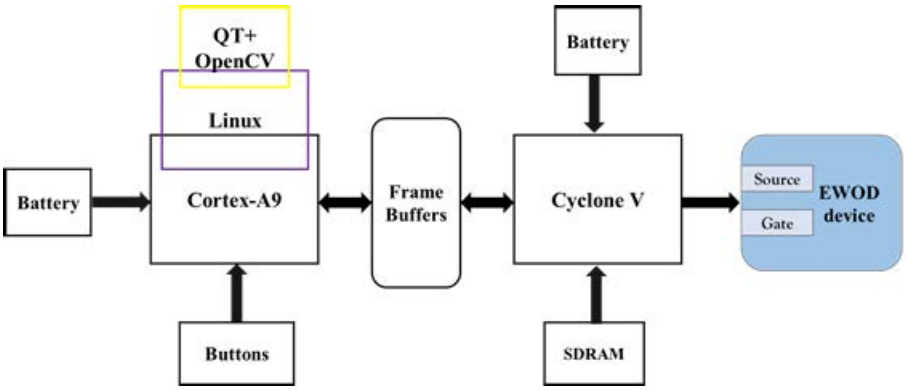

FIGURE 3. Schematic diagram of the proposed portable electronic control system.

device. In the previous research, the authors developed a droplet recognition system based on machine vision for traditional EWOD devices [29]. An adaptive improvement on the droplets detection system has been made based on the version that the author developed before. This system is developed based on OpenCV and QT and can run on a PC platform and electronic control system. For machine vision-based droplet detection systems, three key modules (i.e., image acquisition, image analysis and recognition, droplet position and feedback) need to be designed. When the original image of the TFTA-EWOD device, including droplets, is captured by the camera, an important step is to process this original image through an appropriate image processing scheme. The complete solution for image analysis of the TFTA-EWOD device is shown in Figure 4. We know that the background of the TFTA-EWOD device and the shape of the droplets moving in TFTA-EWOD device have obvious differences. In our scheme, we use the background extraction and droplet extraction algorithm to realize the separation of droplet and TFTA-EWOD Device.

First, the background model of the original image is built by the background subtractor algorithm (K-Near-Neighbour (KNN)) supported by the OpenCV library. This algorithm can extract the background of the original image. Next, morphology is used to analyse the processed TFTA-EWOD device image and explore effective ''expansion'' coefficients. A median-based Gaussian weighted filter (MGWF) that is effective for image edge filtering is developed in droplets detection system. In the image smoothing phase, we propose an improved adaptive filtering (IAMF) algorithm that can effectively eliminate salt-and-pepper noise. Then the locations of droplets in TFTA-EWOD device are recognized by Hough Circles and Hough Lines detection algorithm supported by OpenCV library.

The droplets detection system is mainly responsible for TFTA-EWOD device state identification and droplet control logic. Several droplet operations (e.g., continuous motion, merge) can be automatically manipulated by droplets detection system based on droplet location and feedback.

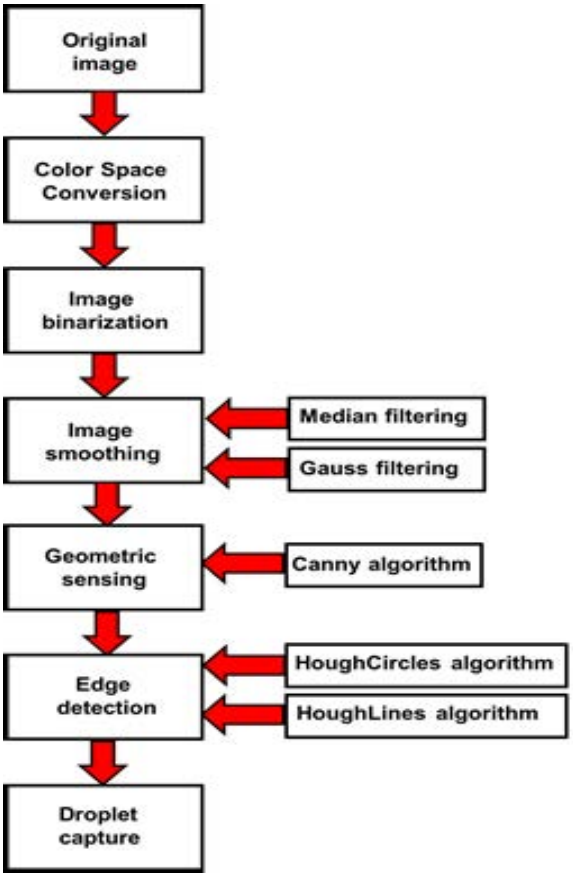

FIGURE 4. Complete solution of image processing and analysis.

III. RESULTS AND DISCUSSIONS

A. DROPLET MOTION EXPERIMENT: SHUTTLING

In this section, different droplet operations are demonstrated and shown with droplets of various sizes and constitutions in the proposed TFTA-EWOD device. The TFTA-EWOD device is capable of manipulating some droplets of different shape simultaneously on account of each electrode is independently switchable. In this experiment, the droplet is shuttled in a TFTA-EWOD device composed of

FIGURE 5. (a) A series of images of droplet manipulation on an EWOD chip. (b) Droplet position results detected by the developed droplet detection system. (c) The position results displayed on the user control interface.

76800 driving electrodes. Shuttling signifies that the droplet is transported forth and back on a TFTA-EWOD device many times.

In traditional EWOD devices, the droplet moves one electrode at a time. However, droplets move through more than one electrode at a time in the TFTA-EWOD device. The ability to control the actuation voltage at small droplet resolution facilitates improved droplet dynamics. For our device, the driving voltage used to actuate the droplet is 20 – 30 V.

A series of images of droplet manipulation (moving) on a TFTA-EWOD device are shown in Figure 5 (a). The parent droplet in this experiment had a volume of 5.6 μL. The premise of precise droplet control is to obtain the real-time droplet position. Droplet detection software based on machine vision could successfully detect the location and

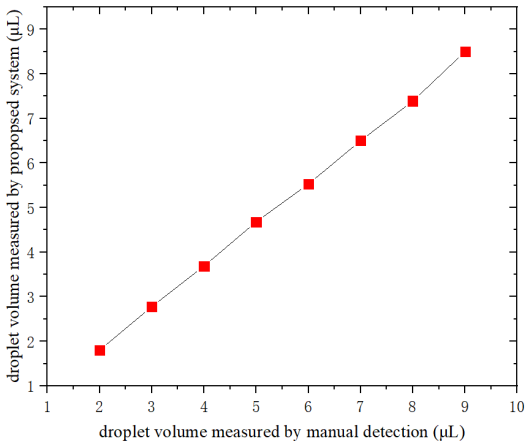

FIGURE 6. Measurement results of droplet volume manually and by the proposed droplet detection system.

shape of the droplet (as shown in Figure 5(b)). Then, the droplet information is transmitted and displayed on the user control interface (Figure 1). 5(c)). The experimental results show that the droplet can shuttle smoothly in the proposed TFTA-EWOD device.

It is known that the droplet size should be larger than the diameter of an electrode element [30], [31] (for our device, it is 150 μm). Below this threshold, the droplet does not move continuously [32]. This means that the minimum volume of droplets operating in the proposed device is approximately 3 nL. Such volume and size are more maneuverable, i.e., larger droplets that encompass several electrode elements, typically 10 or more. This helps to reduce the possibility of operation failure (e.g., the droplet is stuck) due to the droplet being slightly smaller than the electrode elements. In addition, the proposed TFTA-EWOD device has the advantages of a large format and high integration. These advantages are beneficial to the creation and manipulation of droplets of different shapes and volumes.

B. DROPLET VOLUME MEASUREMENT AND CALCULATION

The droplet detection system has the function of droplet volume measurement. The droplet volume measurement module is implemented in the proposed droplet detection system. In this experiment, different volume droplets (Resistivity: 12.5 MΩ, static contact angle: 116°) are measured and calculated by our system. Meanwhile, we used a CCD camera through the microscope for observation. Then, the comparison was made by manual measurement. To ensure the accuracy of the experiment, different volume droplets are driven to different positions within the device array for each measurement. Each case was repeated 3 times. The experimental results are shown in Figure 6.

It can be observed from this experiment that the measurement accuracy of the proposed droplet detection system reaches 90% when the droplet volume is below 5 μL. As the droplet volume increases, the detection error increases slightly. The reason is that the increase in droplet volume leads to an increase in droplet height. When the height of the droplet is much higher than that of the TFTA-EWOD device, the droplet deforms due to extrusion. In this case, the system calculation exhibits a small error. In addition, the system will have slight error (slightly larger) in calculating the volume of liquid with high static contact angle. Because the algorithm uses the elliptic cylinder model to deduce the droplet volume. In general, the experimental results of both measuring methods (manual and system) are found to be in agreement.

C. DROPLET MOTION EXPERIMENT: MERGING

In this section, we attempt to manipulate and track two droplets fusion on the proposed TFTA-EWOD device. Droplet merging is the main function of EWOD device, which is often used in chemical reaction. Merging is identified as a droplet manipulation in which several independent droplets are actuated to move a region for fusion and then the merged large droplet can be transported successfully.

A frequently-used chemical reaction is realized in the TFTA-EWOD device. Figure 7(a) shows molecular components in droplets. The experimental purpose is to discuss the proposed TFTA-EWOD device and matching system performance when multiple droplets move and the droplet volume changes. At the beginning, the volume of the droplet on the left is approximately 2.8 μL and that on the right is 4 μL. The left droplet contains D-glucose. The right one contains NaCl. When they merge in our device, they turn into a large droplet containing D-glucose and NaCl. The volume of the merged droplet is theoretically close to the sum of the two droplet volumes. After the two droplets have merged (as shown in Figure 7(b)), the droplet detection system deduces that the volume of the merged droplets is approximately 7.02 μL. From this experiment, we can see that the measured value of the merged droplet volume is in good agreement with the theoretical value.

The whole merging duration of the two droplets is approximately 18 s. Time-consuming is within the acceptable range. At the same time, we repeat this experiment with no feedback drive mode (only keep the drive module). Under the condition that the droplets can move successfully every time they are driven, the whole merging duration is approximately 15 s. There is no significant increase in merging duration. From the experimental results, we found that the duration of two droplets merging on the proposed TFTA-EWOD is acceptable and comparable with that of other EWOD devices (fabricated by the authors before [33]). It should be noted that the rapid movement of droplet can accelerate the chemical reaction rate. It is similar to shaking a reagent bottle to speed up the chemical reaction rate. This is one of the unique advantages of EWOD devices for DMF system in biological and engineering fields.

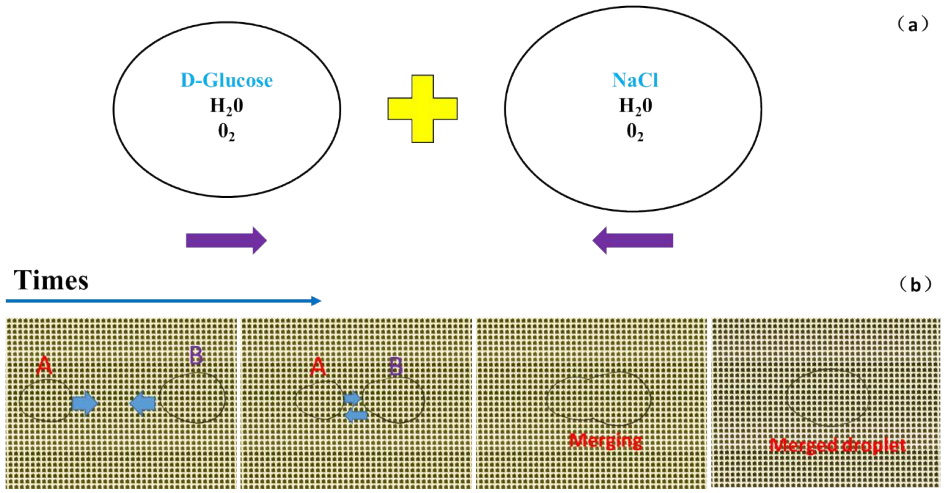

FIGURE 7. A series of images of two droplets merging. (a) The molecular components in two droplets. (b) A sequence of real-time images captured by the camera showing two heterogeneous droplets merging.

D. DROPLET STATUS DETECTION

We evaluated and tested the proposed TFTA-EWOD device and control system by assessing different liquids motion effects in addition to merging and shuttling. We used DI water, PBS, and HBSS as fluids for this experiment. All of them are generally used in field of biological analysis and chemical synthesis. In this detection experiment, different droplets were driven to transport on the same path of the same TFTA-EWOD device.

In EWOD device, the velocity of liquid drop was measured for each droplet motion. It is the ratio between the electrode length (L) and the electrode activation time (T_d) (i.e., $V = L/T_d$) in the absence of feedback model. However, for our droplets detection system, it takes some time (T_i) for image analysis and droplet recognition. T_i is approximately 180 ($\pm$30) ms after repeated testing. In addition, the actuated voltage (T_v) output time is approximately 15 ms.

Hence, in our scheme, the droplet velocity can be calculated as following :

$$V = \frac{L \times D_m}{K_d \times (T_d + T_i + T_v)}$$

where K_d is the number of electrode actuations and D_m is the number of electrodes that the liquid drop actually moves in the TFTA-EWOD device.

Different liquids motion performance (number of successful movement) on the TFTA-EWOD device without a feedback control mechanism is shown in Figure 8. Previous experimental experience tells us that T_d not only determines the effect of droplet motion but also influences the droplet motion velocity in EWOD device. To test the universality of proposed scheme, HBSS, PBS, and DI water were driven across a TFTA-EWOD device at different motion velocities (i.e., different electrode activation times: 300, 500, 800, 1200, 1500, and 1800 ms) with 5 repetitions for a total of 50 actuations.

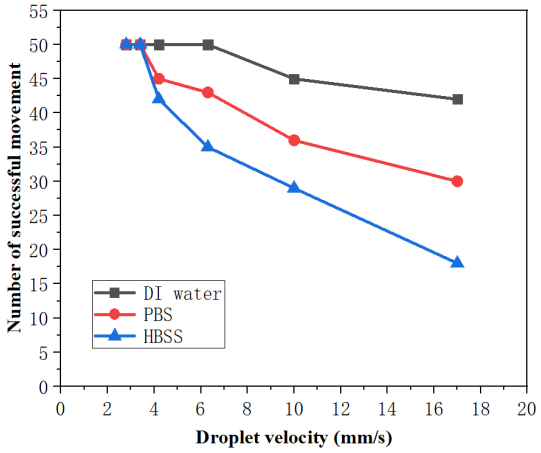

FIGURE 8. Different liquids motion performance on the proposed TFTA-EWOD device without a feedback control mechanism.

From the experimental results, we can see that DI water can achieve a better motion performance in case of high velocities (i.e., 10mm/s and 17 mm/s). However, those liquids containing NaCl (PBS and HBSS) show a poor droplet motion result at higher velocities (i.e., 6mm/s, 10mm/s and 17 mm/s). A longer single electrode activation time may improve the droplet movement performance, but it may aggravate surface fouling of the hydrophobic layer [34]. In addition, a longer single electrode activation time will decrease the practicability of the EWOD chip due to complex droplets path planning.

Droplet status detection experiment reveals that it is inappropriate to apply a fixed electrode activation time to actuate droplet to move on a TFTA-EWOD device. Therefore, the flexible feedback control mechanism is an important part of DMF system. Different from traditional EWOD devices, the proposed TFTA-EWOD device has a large number of electrodes and a small electrode size. If we use

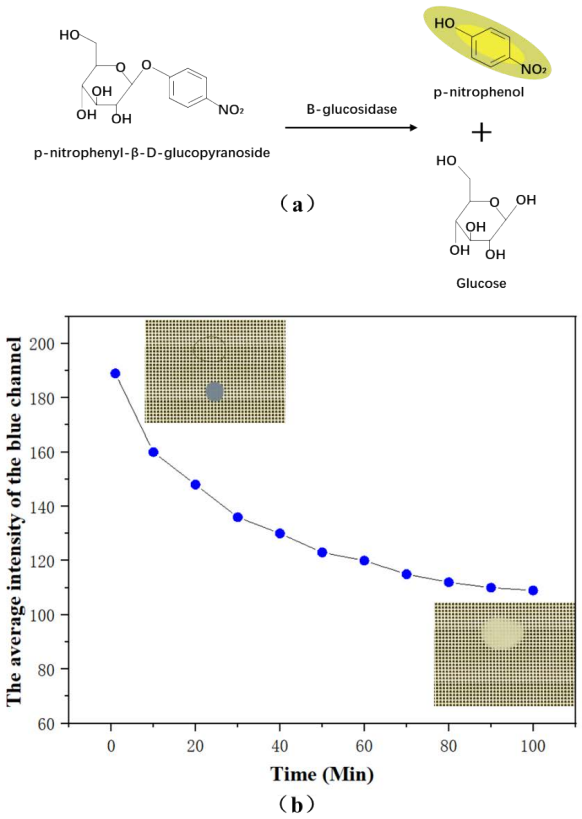

FIGURE 9. β-Glucosidase enzymatic assay using the proposed EWOD device and system. (a) Chemical scheme for this experiment. (b) The average intensity curve of the blue channel as a function of time.

impedance measurement as a droplet tracking mechanism, the efficiency and location accuracy of the DMF system are greatly affected because it usually takes 300-600 ms to collect the equivalent capacitance of an electrode. In addition, the impedance measurement scheme needs more sensors because the capacitance acquisition chip generally has only five channels (i.e., one channel corresponds to one electrode). Compared to different droplet control strategies, we consider that a machine-vision based position and feedback control strategy has good stability and universality. It has good theoretical and practical value for a high-resolution and large-format TFTA-EWOD device.

E. β-GLUCOSIDASE ENZYMATIC ASSAY

To demonstrate the application effect of the TFTA-EWOD device and matching system, we applied our device and system to the β-glucosidase enzymatic assay. We detected the activity of the β-glucosidase enzyme, which is useful for the outcome of biofuels. The classical model for analysing the kinetics of a β-glucosidase enzyme is to use the chromogenic model substrate para-nitrophenyl-β-glucoside (pNPG), which produces para-nitrophenol and glucose (pNP) [35]. The liberation of pNP is a yellow product (in our experiment, it is a yellow droplet) that can be detected by our droplet detection system. The chemical scheme of this experiment is shown in Figure 9(a).

For this experiment, we first identify the region of the droplet through image recognition. A region of interest (ROI) containing a merged droplet is selected. Then, the droplet detection system analyses the RGB profile of the ROI and calculates the average pixel intensities for the RGB (red, green and blue) channel. The green channel of pixels does not show any significant difference when the yellow component of the pixel increases. The red channel changes by approximately 100. Then, the blue channel shows an apparent divergence in the pixel deconstruction of the yellow product (in this experiment, it is pNP). Therefore, we can detect the activity of the β-glucosidase enzyme by tracking the average intensity change of the blue channel in the ROI region. The average intensity curve of the blue channel as a function of time is shown in Figure 9(b). For this experiment, the system measurement interval for the average intensity of the blue channel is 10 min. At the beginning of the chemical reaction, the average intensity curve of the blue channel is approximately 189. It decreases over time. The detection experiment was repeated in triplicate on the same TFTA-EWOD device, and the error bars are ±1.2 SD.

F. EXPERIMENTAL INTERPRETATION AND DISCUSSION

The object of the proposed scheme is to explore and demonstrate the feasibility of using TFTA backplane as DMF platforms for different chemical applications. A source IC and gate IC are bonded on the substrate glass of the device as a driver chip. A TFTA-EWOD device with 320 × 240 electrodes is designed, fabricated and tested in our experiments.

Furthermore, a matching droplet control system based on machine vision with detection and feedback functions was developed and implemented. A flexible feedback control mechanism is provided in the droplet detection system. The droplet detection system provided a 2D graphic interface based on QT to view the detection results

The experimental results show that applying the proposed TFTA-EWOD device and droplet detection system allowed for moving, merging different liquids and analysing the product of chemical reactions. Additionally, tracking the droplet by image recognition and analysis has been demonstrated to be feasible and efficient.

Several special cases were encountered during our experiments. The first issue concerns the drying up and volatilization of the small droplet during experiments. Because the environment of the droplet in the EWOD device is air, this is unavoidable. Another issue is the damage to the lower plate surface in the proposed device. Excessive driving voltage leads to the degradation of the hydrophobic layer. If it is serious, the device burns out. If the surface of the EWOD device may become hydrophilic during the experimental process, a thin layer of Teflon can be deposited by CHF3 plasma using reactive ion etching equipment.

Finally, there are thousands of microelectrodes in the TFTA-EWOD device. Access and individual control of each electrode will be necessary in further development.

IV. CONCLUSION

In this paper, we have demonstrated a programmable high integration and resolution TFTA-EWOD device. A TFTA backplane with thousands of individually addressable electrodes used in an EWD is integrated in this device. The proposed device has many advantages compared with conventional EWOD devices. First, our TFTA-EWOD device has high resolution and a large format. This design allows μm scale droplets manipulation. Smaller droplet sizes and more electrodes can realize complex droplet operations. A source IC and gate IC are integrated on the substrate glass of the device as a driver chip. The proposed device does not need an additional high voltage source or circuit. Users can provide simple control signals that can be generated on a PC or in embedded platforms to realize various droplet operations in our device. Furthermore, a matching droplet control system based on machine vision was developed in this study. This detection system is capable of capturing multiple independent droplets moving and merging failures and integrating a feedback control model while several droplets are simultaneously manipulated on our TFTA-EWOD device.

The experimental results show that different droplet manipulations (i.e., moving, merging, splitting) can be successfully operated in our device. To show the utility of our scheme, we successfully applied the proposed device and system to conduct an enzymatic assay without requiring any other external sensors. Compared with a conventional EWOD device, no additional defects were introduced by the proposed TFTA-EWOD device. The proposed device provides a programmable high integration and high resolution solution for complex fluid manipulation whose performance exceeds that of conventional EWOD devices. We expect that the proposed device and system may be helpful to researchers who are investigating intelligent detection or control platforms for a series of EWOD device applications.

CONFLICT OF INTERESTS

The authors declare that there are no conflicts of interest regarding the publication of this paper.

REFERENCES

[1] N. Shembekar, C. Chaipan, R. Utharala, and C. A. Merten, "Droplet-based microfluidics in drug discovery, transcriptomics and high-throughput molecular genetics," *Lab Chip*, vol. 16, no. 8, pp. 1314–1331, 2016.

[2] D. Mark, S. Haeberle, G. Roth, F. von Stetten, and R. Zengerle, "Microfluidic lab-on-a-chip platforms: Requirements, characteristics and applications," *Chem. Soc. Rev.*, vol. 39, no. 3, pp. 1153–1182, 2010.

[3] D. Weibel and G. Whitesides, "Applications of microfluidics in chemical biology," *Current Opinion Chem. Biol.*, vol. 10, no. 6, pp. 584–591, Dec. 2006.

[4] M. Washizu, "Electrostatic actuation of liquid droplets for micro-reactor applications," *IEEE Trans. Ind. Appl.*, vol. 34, no. 4, pp. 732–737, Jul. 1998.

[5] Z. Guttenberg, H. Müller, H. Habermüller, A. Geisbauer, J. Pipper, J. Felbel, M. Kielpinski, J. Scriba, and A. Wixforth, "Planar chip device for PCR and hybridization with surface acoustic wave pump," *Lab Chip*, vol. 5, no. 3, pp. 308–317, 2005.

[6] J. K. Stark and M. A. Rother, "The combined effects of gravitational and thermocapillary driving forces on the interactions of slightly deformable, Surfactant–Free drops," *Microgr. Sci. Technol.*, vol. 32, no. 3, pp. 399–413, Jun. 2020.

[7] A. N. Banerjee, S. Qian, and S. W. Joo, "High-speed droplet actuation on single-plate electrode arrays," *J. Colloid Interface Sci.*, vol. 362, no. 2, pp. 567–574, Oct. 2011.

[8] T. Mulla and S.-B. Choi, "An electromechanical model of an electro-responsive liquid droplet actuator for microsystems: Modeling and verification," *Sens. Actuators A, Phys.*, vol. 285, pp. 338–347, Jan. 2019.

[9] M. Torabinia, A. Farzbod, and H. Moon, "Electromechanical model to predict the movability of liquids in an electrowetting-on-dielectric microfluidic device," *J. Appl. Phys.*, vol. 123, no. 15, Apr. 2018, Art. no. 154902.

[10] Q. Zhu, Y. Lu, S. Xie, Z. Luo, S. Shen, Z. Yan, M. Jin, G. Zhou, and L. Shui, "Intelligent droplet manipulation in electrowetting devices via capacitance-based sensing and actuation for self-adaptive digital microfluidics," *Microfluidics Nanofluidics*, vol. 24, no. 8, Aug. 2020.

[11] J. Li, S. Chen, and C.-J. Kim, "Low-cost and low-topography fabrication of multilayer interconnections for microfluidic devices," *J. Micromech. Microeng.*, vol. 30, no. 7, Jul. 2020, Art. no. 077001.

[12] I. Ertugrul and O. Ulkir, "Dielectrophoretic separation of platelet cells in a microfluidic channel and optimization with fuzzy logic," *RSC Adv.*, vol. 10, no. 56, pp. 33731–33738, Sep. 2020.

[13] I. Ertugrul, "Modeling of microfluidics chip systems with COMSOL," in *Proc. Int. Conf. Multidisciplinary Sci. (ICOMUS)*, May 2020, pp. 1–5.

[14] I. Unalli, S. Ersoy, and I. Ertugrul, "Microfluidics chip design analysis and control," *J. Mechatronics Artif. Intell. Eng.*, vol. 1, no. 1, pp. 2–7, Jun. 2020.

[15] C. Lee, G.-B. Lee, H.-H. Liu, and F.-C. Huang, "MEMS-based temperature control systems for DNA amplification," *Int. J. Nonlinear Sci. Numer. Simul.*, vol. 79, no. 6, pp. 215–218, 2011.

[16] N. Vergauwe, D. Witters, F. Ceyssens, S. Vermeir, B. Verbruggen, R. Puers, and J. Lammertyn, "A versatile electrowetting-based digital microfluidic platform for quantitative homogeneous and heterogeneous bio-assays," *J. Micromech. Microeng.*, vol. 21, no. 5, May 2011, Art. no. 054026.

[17] H.-H. Shen, S.-K. Fan, C.-J. Kim, and D.-J. Yao, "EWOD microfluidic systems for biomedical applications," *Microfluidics Nanofluidics*, vol. 16, no. 5, pp. 965–987, May 2014.

[18] G. S. Du, J.-Z. Pan, S.-P. Zhao, Y. Zhu, J. M. J. den Toonder, and Q. Fang, "Cell-based drug combination screening with a microfluidic droplet array system," *Anal. Chem.*, vol. 85, no. 14, pp. 56–65, 2013.

[19] W. Cui, M. Zhang, X. Duan, W. Pang, D. Zhang, and H. Zhang, "Dynamics of electrowetting droplet motion in digital microfluidics systems: From dynamic saturation to device physics," *Micromachines*, vol. 6, no. 6, pp. 778–789, Jun. 2015.

[20] Y. Guan, B. Li, M. Zhu, S. Cheng, and J. Tu, "Deformation, speed, and stability of droplet motion in closed electrowetting-based digital microfluidics," *Phys. Fluids*, vol. 31, no. 6, pp. 062002–062008, 2019.

[21] M. K. Ahmadi, M. Shokoohi, and M. Passandideh-Fard, "Experimental characterization of droplet dispensing in electrowetting-based microfluidics," *Appl. Phys. Lett.*, vol. 111, no. 4, pp. 547–555, 2017.

[22] M. A. Murran and H. Najjaran, "Capacitance-based droplet position estimator for digital microfluidic devices," *Lab Chip*, vol. 12, no. 11, pp. 2053–2059, 2012.

[23] J. H. Noh, J. Noh, E. Kreit, J. Heikenfeld, and P. D. Rack, "Toward active-matrix lab-on-a-chip: Programmable electrofluidic control enabled by arrayed oxide thin film transistors," *Lab Chip*, vol. 12, no. 2, pp. 353–360, 2012.

[24] B. Hadwen, G. R. Broder, D. Morganti, A. Jacobs, C. Brown, J. R. Hector, Y. Kubota, and H. Morgan, "Programmable large area digital microfluidic array with integrated droplet sensing for bioassays," *Lab Chip*, vol. 12, no. 18, pp. 3305–3313, 2012.

[25] F. A. Shaik, G. Cathcart, S. Ihida, M. Lereau-Bernier, E. Leclerc, Y. Sakai, H. Toshiyoshi, and A. Tixier-Mita, "Thin-film-transistor array: An exploratory attempt for high throughput cell manipulation using electrowetting principle," *J. Micromech. Microeng.*, vol. 27, no. 5, pp. 054001–054011, 2017.

[26] Y. Li, H. Li, and R. J. Baker, "A low-cost and high-resolution droplet position detector for an intelligent electrowetting on dielectric device," *J. Lab. Automat.*, vol. 20, no. 6, pp. 1–7, 2015.
[27] C. Elbuken, T. Glawdel, D. Chan, and C. L. Ren, "Detection of microdroplet size and speed using capacitive sensors," *Sens. Actuators A, Phys.*, vol. 171, no. 2, pp. 55–62, Nov. 2011.
[28] V. Jain, A. Hole, R. Deshmukh, and R. Patrikar, "Dynamic capacitive sensing of droplet parameters in a low-cost open EWOD system," *Sens. Actuators A, Phys.*, vol. 263, pp. 224–233, Aug. 2017.
[29] Z. Luo, B. Huang, J. Xu, L. Wang, Z. Huang, L. Cao, and S. Liu, "Machine vision-based driving and feedback scheme for digital microfluidics system," *Open Chem.*, vol. 19, no. 1, pp. 665–677, Jun. 2021.
[30] S. K. Fan, T. H. Hsieh, and D. Y. Lin, "General digital microfluidic platform manipulating dielectric and conductive droplets by dielectrophoresis and electrowetting," *Lab Chip*, vol. 9, no. 9, pp. 1236–1242, 2009.
[31] M. G. Pollack, A. D. Shenderov, and R. B. Fair, "Electrowetting-based actuation of droplets for integrated microfluidics," *Lab Chip*, vol. 2, no. 2, pp. 96–102, 2002.
[32] L. Clime, D. Brassard, and T. Veres, "Numerical modeling of electrowetting transport processes for digital microfluidics," *Microfluidics Nanofluidics*, vol. 8, no. 5, pp. 599–608, May 2010.
[33] Z. Luo, J. Fan, B. Huang, S. Liu, and F. Dai, "Position and feedback for digital microfluidic system based on light intensity information," *Asia–Pacific J. Chem. Eng.*, vol. 15, no. S1, Sep. 2020.
[34] R. S. Hale and V. Bahadur, "Electrowetting-based microfluidic operations on rapid-manufactured devices for heat pipe applications," *J. Micromech. Microeng.*, vol. 27, no. 7, Jul. 2017, Art. no. 075004.
[35] P. Q. N. Vo, M. C. Husser, H. Sinha, F. Ahmadi, and S. C. C. Shih, "Image-based feedback and analysis system for digital microfluidics," *Lab Chip*, vol. 17, no. 20, pp. 3437–3446, 2017.

ZHIJIE LUO graduated from South China Normal University, in 2017. He received the Ph.D. degree in electronic science. He worked with the Zhongkai University of Agriculture and Engineering. He is currently a Lecturer. His research interests include digital microfluidic systems and EWOD displays.

JIAZHI XU received the bachelor's degree from the Zhongkai University of Agriculture and Engineering. His research interest includes electronic system design.

ZHONGYU PAN received the bachelor's degree from the Zhongkai University of Agriculture and Engineering. His research interest includes image recognition.

HANG YIN worked with the Zhongkai University of Agriculture and Engineering. He is currently an Associate Professor. His research interest includes machine artificial intelligence algorithm.

LIANG CAO worked with the Zhongkai University of Agriculture and Engineering. He is currently a Lecturer. His research interests include machine learning and software design.

GUOFU ZHOU is currently the Founder and the Director of the Electronic Paper Display Institute, South China Normal University, Guangzhou, China, and a part-time Professor at the Department of Electrical Engineering, Eindhoven University of Technology, Eindhoven, The Netherlands. He holds more than 100 scientific publications and is an inventor of more than 100 patents in the field of optoelectronic micro/nano materials, devices, and systems. As recognition, he is awarded with the Gold Medal ISMANAM-1994 Grenoble and 2006 Gilles Holst Award of Royal Dutch Philips.

SHUANGYIN LIU graduated from China Agricultural University, in 2014. He worked with the Zhongkai University of Agriculture and Engineering. He is currently a Professor. His research interests include machine learning and big data processing.